Anal Bioanal Chem
DOI 10.1007/s00216-009-3332-5

REVIEW

Chemical and structural characterization of carbon nanotube surfaces

Kevin A. Wepasnick · Billy A. Smith · Julie L. Bitter · D. Howard Fairbrother

Received: 3 September 2009 / Revised: 18 November 2009 / Accepted: 19 November 2009

Abstract To utilize carbon nanotubes (CNTs) in various commercial and scientific applications, the graphene sheets that comprise CNT surfaces are often modified to tailor properties, such as dispersion. In this article, we provide a critical review of the techniques used to explore the chemical and structural characteristics of CNTs modified by covalent surface modification strategies that involve the direct incorporation of specific elements and inorganic or organic functional groups into the graphene sidewalls. Using examples from the literature, we discuss not only the popular techniques such as TEM, XPS, IR, and Raman spectroscopy but also more specialized techniques such as chemical derivatization, Boehm titrations, EELS, NEXAFS, TPD, and TGA. The chemical or structural information provided by each technique discussed, as well as their strengths and limitations. Particular emphasis is placed on XPS and the application of chemical derivatization in conjunction with XPS to quantify functional groups on CNT surfaces in situations where spectral deconvolution of XPS lineshapes is ambiguous.

Keywords X-ray spectroscopy (XPS | XRF | EDX) · Nanoparticles/nanotechnology · Spectroscopy/instrumentation · Potentiometry/titrations · IR spectroscopy/Raman spectroscopy · Interface/surface analysis

K. A. Wepasnick · B. A. Smith · J. L. Bitter · D. Howard Fairbrother (✉)
Department of Chemistry, Johns Hopkins University, Baltimore, MD 21218, USA
e-mail: howardf@jhu.edu

D. Howard Fairbrother
Department of Materials Science and Engineering, Johns Hopkins University, Baltimore, MD 21218, USA

Introduction

A carbon nanotube (CNT) is a hexagonal array of carbon atoms rolled up into a long, thin, hollow cylinder [1]. Two structural forms of CNTs exist: single-walled (SWCNTs) and multi-walled (MWCNTs) nanotubes. CNT lengths can be as short as a few hundred nanometers or as long as several microns. SWCNT have diameters between 1 and 10 nm and are normally capped at the ends. In contrast, MWCNT diameters are much larger (ranging from 5 nm to a few hundred nanometers) because their structure consists of many concentric cylinders held together by van der Waals forces [2, 3]. CNTs have extremely high surface areas, large aspect ratios, remarkably high mechanical strength (e.g., tensile strengths 100 times greater than that of steel) and electrical and thermal conductivities that are similar to that of copper [4, 5].

The desirable materials properties of CNTs have already resulted in their incorporation into a number of consumer products, such as reinforcements for polymer composites [6] and high power-density anodes in Li ion batteries [7]. It is also expected that CNT-based field-effect transistors will soon supplant silicon-based analogs [8]. Between 2006 and 2007, the estimated global market value for CNTs increased from $59.9 to $79.1 million. By 2011, their market value is expected to have increased 10-fold compared with present day values [9].

Despite their many desirable properties, the hydrophobicity and chemical inertness of CNTs frequently hinders their commercial utilization. To overcome these limitations, CNT surfaces are often tailored using either covalent or non-covalent modification strategies. Covalent surface modification involves the direct incorporation of new elements (e.g., oxygen, fluorine, nitrogen) or organic functionalities (e.g., biomolecules) into the CNT sidewalls.

Published online: 06 January 2010

The surface properties of CNTs (e.g., dispersion) can also be changed without modifying their intrinsic structure by non-covalent surface modification strategies that include the adsorption of surfactants, polymers, or biological macromolecules [10].

Both covalent and non-covalent modification strategies are used to prepare CNTs for polymer composites [6], electronic devices [7, 8], and medicinal applications [10, 11]. For example, when CNTs are used as polymer reinforcements, their surfaces are modified by addition of polar functional groups that not only improve their dispersion properties in the resin matrix but also provide cross-linking capabilities during polymerization. In electronics applications, covalent modification strategies involving fluorine or nitrogen atom incorporation are often used to alter the CNTs' density of states, which in turn changes their semiconducting properties [8]. In biomedical applications, CNT dispersions are often prepared by covalently or non-covalently functionalizing the CNT with poly(ethylene glycol) (PEG) or other biocompatible molecules [10, 11].

To understand the changes that result from surface modification strategies, accurate characterization of the CNTs' surface chemistry and structure is needed. In this review, we will highlight the strengths and limitations of various analytical techniques used to characterize the structure, chemical composition, and functional groups introduced after covalent modification strategies, where new species are chemically attached or grafted into the CNT sidewalls. We then use examples from the literature to illustrate how these analytical techniques have been used to study different covalent modification processes.

In this review, we have focused on analytical techniques that can probe surface chemical and structural changes that occur to CNTs as a consequence of covalent modification strategies. As a result, techniques such as atomic force microscopy (AFM) and scanning electron microscopy (SEM), which are capable of measuring CNT lengths and diameters, will not be discussed. Additionally, techniques such as energy-dispersive X-ray spectroscopy (EDX), which can only provide bulk chemical information on CNTs, will only be discussed in passing.

Analytical techniques

A variety of different techniques can be used to characterize the surface chemistry or structure of CNTs after covalent functionalization. Table 1 highlights the most important and widely used methods of analysis. The information provided by each technique, and their strengths and limitations are also summarized. General references describing the physical basis of each technique are also included. At the end of this section, we then briefly describe how some of these analytical techniques can be used to assess CNT purity.

Infrared spectroscopy (IR)

IR spectroscopy can identify organic functional groups on a CNT's surface by measuring characteristic vibrational modes. However, IR does not provide a quantitative measure of functional group concentrations, and peaks are often hard to distinguish from background features. Furthermore, studies in our laboratories have shown that IR spectroscopy lacks the sensitivity to detect some functional groups whose presence have been identified by other analytical techniques.

X-ray photoelectron spectroscopy (XPS)

XPS measures CNT surface composition by determining the binding energy of photoelectrons ejected when CNTs are irradiated with X-rays. The surface sensitivity of XPS is derived from the small (<10 nm) inelastic mean free path of the ejected photoelectrons. This allows the elemental composition (except for hydrogen) of the near surface region to be quantified. One limitation of XPS is that it requires a relatively large amount of sample (~5 mg) because of the comparatively large analysis area required (~10 μm diameter), even for state-of-the-art XP spectrometers.

In addition to compositional analysis, XPS can also provide information on the chemical environment of surface species (e.g., CF vs. CF_2) based on the peak-fitting of XP spectral envelopes. This capability stems from the fact that, although a photoelectron's binding energy (BE) is largely determined by the element from which it originates, BEs are also influenced (to a lesser extent) by the local chemical environment (e.g., for carbon atom: C-F vs. C-C). However, deconvolution of XPS spectral envelopes can be ambiguous.

Chemical derivatization (CD)

As an alternative to peak-fitting, chemical derivatization techniques can be used to quantify the concentration of some functional groups. Derivatization methods have been used previously on plasma-treated polymer surfaces [14], but have only recently been developed to quantify functional groups on other carbonaceous surfaces such as CNTs [19–21]. In CD, a targeted oxygen-containing functional group reacts selectively and stoichiometrically with a specific derivatizing reagent that contains a unique chemical tag. After each derivatization reaction, the concentration of these chemical tags introduced on to the surface can be quantified. Based on this information, the concentration of the targeted functional group can then be determined from knowledge of the chemical reaction that occurs between the targeted functional

Table 1 Applications and limitations of techniques used to analyze the structure and surface chemistry of CNTs

Analytical technique	Information provided/strengths	Limitations	Overview of technique (References)
IR	Functional group identification	Not quantitative, some IR modes are too weak to be observed	[12, 13]
XPS	Surface composition and, in principal, information about functional groups	Requires relatively large amounts of sample (~5 mg), peak-fitting is often ambiguous and over interpreted.	[12, 13]
Chemical derivatization	Direct quantification of targeted functional groups	Not all function groups can be derivatized	[13–15]
Boehm titrations	Quantification of protic functional groups	Does not provide information on aprotic functionalities. Requires large amounts of sample (>10 mg)	[16]
TGA and TPD	Concentration of organic species attached to CNTs	Requires large amount of sample (>10 mg). Data interpretation is often subjective.	[17]
EELS and NEXAFS	Surface composition and functional groups identification	Can be difficult to implement for routine analysis	[12, 13, 18]
TEM	Images of CNTs, observation of sidewalls. CNT diameter, length, and dispersion state can also be determined. Chemical analysis by EDX is also often available in TEMs	CNTs are susceptible to damage from the high-energy electron beam. Sample preparation and drying can result in ambiguous analysis	[12, 18]
Raman spectroscopy	I_D:I_G band ratios can provide a metric of sidewall damage or purity	I_D:I_G band ratio can be misinterpreted or misleading	[12, 13]

group and the derivatizing agent. The concentration of the chemical tags can be quantified either by XPS or another analytical technique, such as fluorescence, depending on the nature of the tag. For CD used in conjunction with XPS, fluorine atoms are often used as the chemical tags because they are not normally present on CNT surfaces; furthermore, the F(1s) core level transition has a high XP cross-section. CD is limited by the same sample size constraints as XPS and by the fact that not all functional groups can be selectively labeled.

Boehm titrations

To determine quantities of protic functional groups (carboxyls, lactones, lactols, and in some cases carbonyls), classical Boehm titrations can be applied. In a Boehm titration, a CNT's protic groups are neutralized with "bases of various basicities" (e.g., $NaHCO_3$, Na_2CO_3, NaOH, $NaOC_2H_5$) [16]. Because the acidity constants (pK_a) of protic functional groups vary by several orders of magnitude, these different bases can determine the concentration of different CNT functional groups. These titrations, however, can only quantify the protic functional groups (e.g., COOH, OH), and therefore, cannot be applied to aprotic functionalities.

Thermogravimetric analysis (TGA) and temperature programmed desorption (TPD)

TGA measures the decrease in sample mass as a function of annealing temperature. Because CNTs generally have higher decomposition temperatures than adsorbed molecules and amorphous carbon, TGA data can be used to estimate CNT purity and the presence and concentration of organic molecules attached to CNT sidewalls. Metal impurities can also be assayed by examining the residual sample mass when all of the organics have been volatilized.

In TPD, the sample is heated under vacuum conditions. Volatile products generated when organic functional groups thermally decompose are analyzed as a function of sample temperature by mass spectrometry. For CNTs, the chemical analysis and quantification of the desorbed species can be used to identify and quantify some surface functional groups.

Because TGA is based on mass change and TPD is based on the intensity of volatile material generated, the resolution and capability of the techniques are dependent on the quantity of CNTs used. These techniques can, therefore, require large amounts of material (>10 mg) for high-quality data. TGA and TPD data is also often difficult to interpret because of the close proximity of different peaks, which gives rise to broad, featureless traces.

Electron energy loss spectroscopy (EELS) and near-edge X-ray absorption fine structure (NEXAFS)

EELS can measure the elemental composition of CNTs by measuring the energy lost by incident electrons as they interact with CNT atoms. This creates an absorption edge at element-specific energies because of core-shell ionization events. The composition of the CNT can be determined by

analyzing the energy and relative intensities of different adsorption edges. Used in conjunction with TEM, EELS can generate elemental maps of a CNT; for example, Čech et al. were able to show the location of sulfur atoms in an MWCNT after thiolation [22]. Routine use of EELS is limited, however, because it requires specialized equipment.

Using a tunable X-ray source, NEXAFS can provide detailed information on local bonding environments associated with different elements by monitoring the electron yield as a function of the incident photon energy. Like EELS, each element creates a number of absorption edges because of core-shell ionizations, and the detailed structure of each edge contains comprehensive structural information on the local bonding environment of the element. The use of NEXAFS for routine analysis is limited by the need for a tunable X-ray source, typically a synchrotron; also, NEXAFS edge spectra can only be reliably interpreted when a few chemical states of an element are present. When a large number of chemical species are present an unambiguous fit to any edge spectrum is extremely difficult because of the close proximity of the various peak positions, similar in many respects to the issues inherent in the spectral deconvolution of XPS lineshapes.

Transmission electron microscopy (TEM)

TEM uses a high-energy electron beam (up to 300 keV) to image CNTs based on electron transmission. The length and dispersion state of CNTs can be assessed by TEM at low magnification. At high magnifications, TEM can be used to count the number of walls in MWCNTs, measure inner and outer diameter, assess structural integrity, and identify structural changes (e.g., sidewall damage) caused by surface modification.

Although TEM is capable of imaging the structure of CNTs, including the presence of sidewall damage, the electrons used for imaging can themselves also cause sidewall damage and structural modification. To avoid this problem it has been recommended that analysis areas only be exposed to the electron beam for very shot durations (<15 s), and that beam energies should be limited to 100 keV [23]. As in many imaging techniques, verification that an observed structure remains unchanged with respect to irradiation time is the best way to ensure that the analysis technique is non-destructive.

Raman spectroscopy

In Raman spectroscopy, vibrational modes are identified by measuring the energy of scattered photons generated from a sample exposed to intense laser light. Raman spectra of CNTs typically consist of a graphitic or G-band, from highly ordered CNT sidewalls, while disorder in the sidewall structure results in a D-band. By determining the ratio between these two bands (I_D:I_G), a quantitative measure of defect density in the CNT sidewall can be determined. Consequently, I_D:I_G band analysis can be used to obtain information regarding structural changes as a result of functionalization. Unfortunately, many CNTs can have amorphous carbon adsorbed on the sidewalls, which also contributes to the D-band. In the absence of amorphous carbon, however, I_D:I_G ratios can be very useful for determining changes in structure that occur as a result of functionalization strategies, such as those that involve the attachment of organic moieties. In the case of SWCNTs, a vibrational mode known as the radial breathing mode (RBM) can also be used to determine the SWCNT's diameter based on its peak position [24].

CNT purity

Determining the purity of CNTs is often an important component of structural and chemical characterization. This because most typical methods of synthesizing CNTs result in is amorphous carbon being present on the CNT surface and residual metal catalyst nanoparticles embedded within the hollow interior. Microscopy techniques such as TEM can directly visualize amorphous carbon on the CNT surface (as shown in Fig. 1) and can also identify residual metal nanoparticles by virtue of differences in their electron transmission properties compared with the majority carbon atoms. Although direct visual inspection and identification is possible, quantitative determination of impurity levels by TEM is challenging [25]. In contrast to TEM, Raman spectroscopy can provide a quantitative metric of adsorbed amorphous carbon, based on the intensity ratio of the D and G-bands. Sidewall defects in CNTs, however, can also contribute spectral intensity to the D-bands, making it difficult to use I_D:I_G band ratios as unambiguous measures of amorphous carbon content unless the structural integrity of the CNT has been independently determined, for example, by TEM. TGA can also quantify purity by measuring the mass loss from a CNT because of thermal desorption of adsorbed amorphous carbon, which, in air, typically desorbs at 400 K, while carbon atoms from CNTs are typically stable up to 500 K [26]. The quantity of remaining trace metal catalysts can also be determined by TGA based upon the residual mass obtained after complete CNT decomposition/volatilization at temperatures greater than 700 K [27]. Bulk measurements of a CNT's chemical composition by EDX can also provide insights into the presence and concentration of trace metal contaminants.

Discussion

In the following sections, we use examples from the scientific literature to illustrate how the analytical techni-

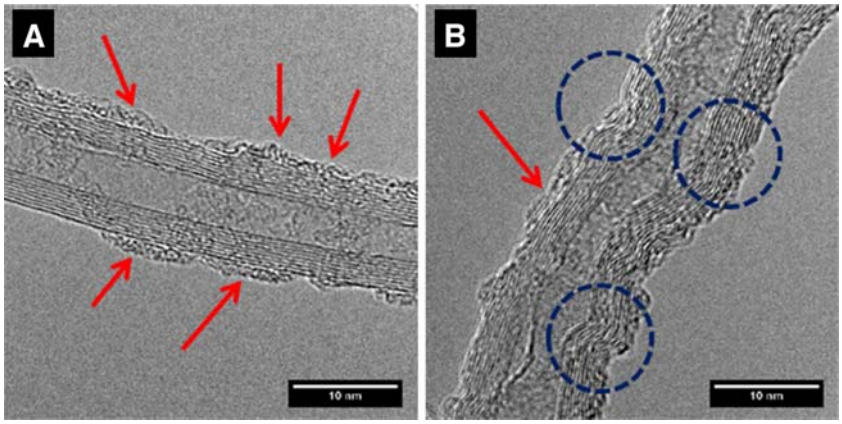

Fig. 1 High resolution TEM images of (**A**) a pristine MWCNT and (**B**) a MWCNT oxidized with H_2SO_4/HNO_3. *Arrows* highlight the presence of amorphous carbon and *circles* indicate locations of sidewall damage

ques described in the previous section have been used to probe the effect of different covalent surface modification strategies, where chemical functionalities have been directly attached to CNT sidewalls. Specifically, we consider strategies that involve the incorporation of oxygen, nitrogen, and fluorine. We then discuss how analytical techniques have been used to analyze organic functional groups and metals attached to CNTs.

Oxygen

The incorporation of oxygen atoms into the CNT surfaces is by far the most common covalent modification. For example, oxygen functional groups are deliberately incorporated into CNTs using various treatment methods (e.g., plasma, oxidation, sonication) to modify dispersion properties [20, 28, 29]. These functional groups can also serve as attachment points in the construction of more complex, multi-functional nanostructured materials [30, 31]. Oxygen functional groups can also be incidentally incorporated after laboratory purification processes used to remove amorphous carbon and residual metal particles, or as a result of CNT exposure to oxidants present in the environment (e.g., O_3) [32, 33].

In our laboratory, we have used XPS to determine the concentration of oxygen incorporated into MWCNTs after treatment with various oxidizing acids (e.g., HNO_3, H_2SO_4/HNO_3, or $KMnO_4$ [29, 34, 35]). XPS analysis has shown that the more aggressive oxidants result in a higher percentage of oxygen incorporation. For example, we have found that the extent of oxygen incorporation varies linearly with the HNO_3 weight percentage used during the oxidation process [29]. After aggressive oxidative treatments, for example H_2SO_4/HNO_3 (Fig. 1b), we also observed with TEM an increase in sidewall damage, as compared with pristine MWCNTs (Fig. 1a). We also observed a concomitant decrease in the quantity of amorphous carbon adsorbed on the CNT surface. While, in principle, Raman spectroscopy could monitor changes in the sidewall damage because of oxidation, the presence of amorphous carbon (also present on our pristine MWCNTs as shown with TEM) renders analysis of the I_D:I_G bands ambiguous. This is a consequence of the fact that CNT oxidation leads to both the removal of amorphous carbon and the introduction of defect sites along the CNT sidewalls, both of which contribute to D-band intensity.

Researchers have used XPS to examine changes in the surface oxygen concentration of CNTs as a result of ozone exposure [32], acid washing [36–38], plasma treatment [20], or sonication [28]. In a related study of purification, Hou et al. used XPS to determine if oxygen or bromine was being incorporated or removed from MWCNTs surfaces in each step of an aggressive purification process which included bromination [33].

Functional group identification with XPS

Using XPS, the identity and concentration of oxygen-containing functional groups formed as a result of CNT oxidation can, in principle, be obtained from spectral deconvolution of the O(1s) or C(1s) XPS regions. Unambiguous spectral deconvolution is, however, often complicated by the presence of different species (e.g., C-H, C-O, C=O, COOH) with similar binding energies. For CNTs, spectral deconvolution of the C(1s) region is further complicated by the presence of a π-π^* shake-up feature that must be taken into account. Furthermore, XPS peak fitting cannot be used to distinguish between oxygen-containing functional groups which have the same binding energy (e.g., alcohols, C-OH vs. ethers, C-O-C). Discrepancies in the literature regarding peak positions and full-width-half-max (FWHM) values of different species significantly add to the complexity of spectral analysis. To illustrate this issue, we have peak fit the C(1s) region of an oxidized MWCNT sample using two different sets of literature values (Li et al. [32] and Wang et al. [39]) for the peak positions of oxygen-containing functional groups (Table 2). The RMS error for both methods (also shown in Table 2) shows that each method

Table 2 C(1s) peak fitting results obtained for H_2SO_4/HNO_3 treated MWCNTs, analyzed using two sets of peak positions (shown in parentheses)

Method	C-C/C=C% (eV)	C-OH% (eV)	C=O% (eV)	COOH% (eV)	π-π*% (eV)	Residual peak area (RMS Value)
Li et al. [32]	44.3 (284.6)	23.1 (285.8)	15.4 (286.8)	11.0 (288.9)	6.2 (292.0)	901[a]
Wang et al. [39]	38.3 (284.6)	26.0 (285.2)	15.4 (286.8)	5.9 (289.1)	10.7 (291.0)	831[a]

[a] For reference, the total area of the C(1s) spectral envelope is 20223

fits the data well with similar levels of error. Despite the relative similarities in the peak positions, Fig. 2 shows that the two methods give rise to different results, particularly with regard to COOH concentrations.

Chemical derivatization (CD)

To overcome the difficulties in deconvoluting the C(1s) (or O(1s)) spectral envelopes, we have used CD-XPS to quantify the surface concentration of three major oxygen-containing functionalities: hydroxyl (C-OH), carbonyl (C=O), and carboxyl (COOH) groups. In three separate reactions, hydroxyl groups are labeled by reaction with trifluoroacetic anhydride, carbonyl by trifluoroethylhydrazine, and carboxyls via a coupling reaction of trifluoroethanol and a carbodiimide (Fig. 3(a–c)). Each derivatization reaction is selective in labeling a single functional group with reaction efficiencies close to unity [40]. Using CD-XPS, we show in Fig. 4 that MWCNTs oxidized with $KMnO_4$ and HNO_3 exhibit greater fractions of COOH functionalities compared with MWCNTs treated with O_3. CD-XPS has also been able to show that COOH functionalities play a determinant role in improving MWCNT colloidal stability [29, 35] and sorption properties towards divalent metal cations [19]. Zschoerper et al. used the same CD-XPS reactions to determine that changes in the

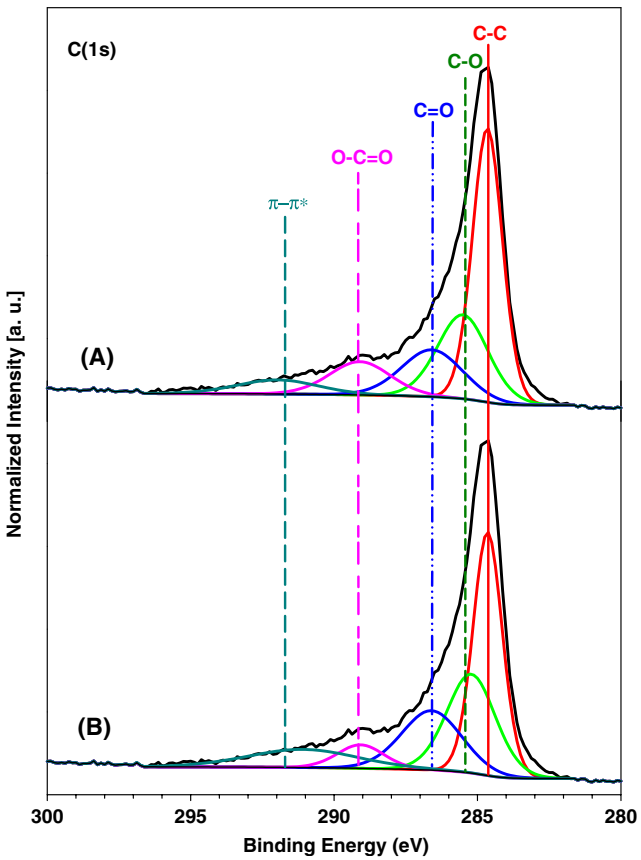

Fig. 2 Peak-fitting results obtained by analyzing the C(1s) region of MWCNTs treated with H_2SO_4/HNO_3 using peak positions from (**A**) Li et al. [32] and (**B**) Wang et al. [39] In (A) and (B), five different spectral features were used to fit the C(1s) envelope: unmodified carbon (C-C), three oxygen-containing environments (C-O, C=O, O-C=O), and π-π* shakeup features. Peak positions are indicated in Table 2

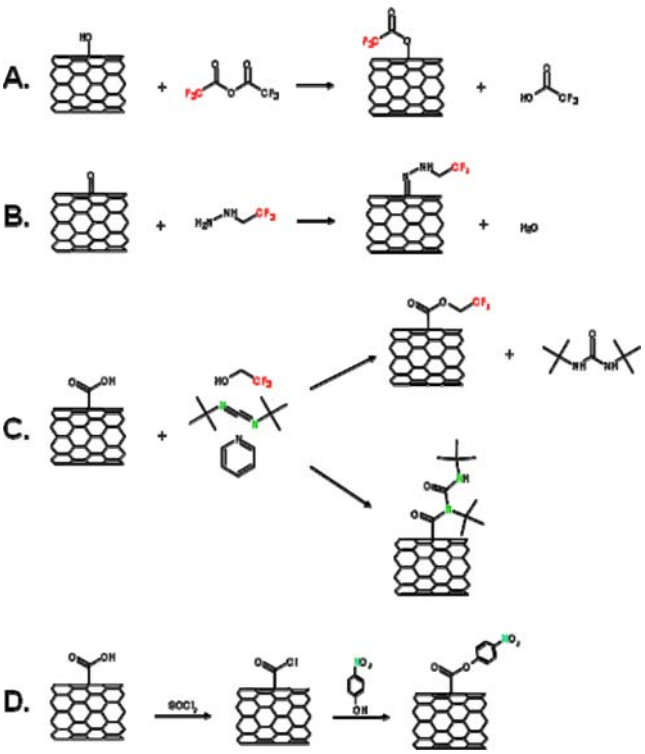

Fig. 3 Reactions schemes for derivatizing oxygen containing functional groups on the surface of CNTs; (**A**) hydroxyl groups with trifluoroacetic anhydride, (**B**) carbonyl groups with trifluoroethylhydrazine, (**C**) carboxylic acid groups with trifluoroethanol and di-*tert*-butyl carbodiimide, and (**D**) carboxylic acid groups in a two-step process using $SOCl_2$ and then 4-nitrophenol

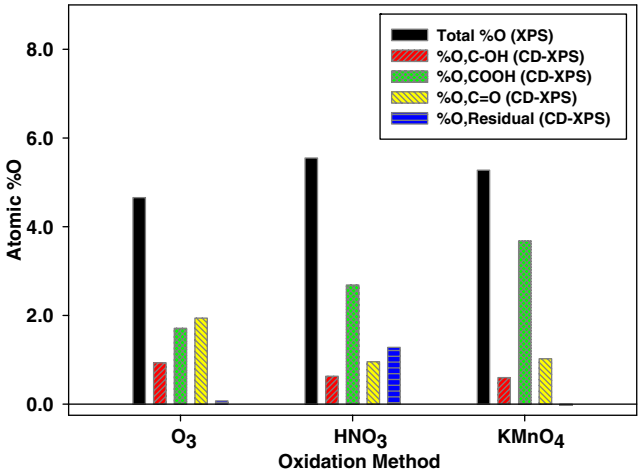

Fig. 4 Oxygen-containing functional group distributions as determined by chemical derivatization (CD-XPS) for MWCNTs treated with O_3, HNO_3, and $KMnO_4$. Residual refers to oxygen-containing functional groups which cannot be derivatized (e.g., ester, ethers, lactones). Total oxygen concentration (*black*) was determined by simple XPS elemental analysis

treatment times and conditions (e.g., pressure) of an Ar/O_2 or Ar/H_2O plasma effect the quantitative distribution of surface oxides [20]. They noted that both plasma treatments resulted in a disproportionally large increase in the C=O functional group concentration, and that lower pressures tended to produce the greatest increase in overall carboxyl, hydroxyl, and carbonyl functional group concentrations.

In a study by Masheter et al., COOH groups were derivatized using a two-step process that involved first forming an acid chloride followed by a nucleophilic substitution reaction with 4-nitrophenol (Fig. 3d) [41]. Analysis of the N(1s) region by XPS, with changes in the voltammetric properties of different SWCNTs and MWCNTs were used to measure increases in COOH group concentration after H_2SO_4/HNO_3 treatment [41].

Another method for chemically derivatizing oxygen-containing functional groups involves labeling carboxyl, hydroxyl, and carbonyl surface species with fluorescent tags [21]. In many ways, fluorescent labeling is complementary to CD-XPS; the fluorescent tags can enable lower concentrations of oxygen functional groups to be detected. However, at higher oxygen functional group concentrations, the bulky fluorescent chromophores are more likely to encounter problems associated with steric hindrance, making quantitative analysis more difficult.

NEXAFS has also been used to elucidate the oxygen functional groups incorporated into SWCNTs following acid purification by H_2SO_4/HNO_3. The oxygen concentration was found to be ~6 at. %, and based on π*(C=O) and σ*(C-O) resonances in the carbon K-edge, carbonyl and ether functional groups were identified [42]. Upon heating to 500 K, the concentration of carbonyl groups decreased. At 1073 K, all the carbonyl and ether groups were removed, along with almost all (~90%) of the oxygen atoms [42].

The concentration of protic oxygen functional groups on CNT sidewalls can also be measured by use of Boehm titrations. Li et al. [43] and Wang et al. [39] used Boehm titrations to assess the quantity of protic groups on acid-washed MWCNT surfaces. Using this information, they were able to show that carboxyl groups played a determinant role in the sorption of Cd(II) and Pb(II) [39, 43].

The various spectroscopic methods described so far are capable of analyzing the concentration of different functional groups produced when CNTs are oxidized. However, a number of non-spectroscopic methods can assay the COOH group concentration. For example, TPD can be used to determine the concentration of surface carboxyl groups on MWCNTs, by measuring the concentration of CO_2 produced during COOH decarboxlyation at ~400 °C [36]. In the same study, NH_3 absorption with TPD was used to determine the COOH group concentration by measuring the peak area associated with a high-temperature shoulder in the NH_3 desorption trace. This high-temperature feature corresponds to ammonia molecules chemisorbed to COOH groups in the form of ammonium carboxylates. The total uptake of ammonia was determined to be 4 mmol g^{-1}, which approximately correlated to the COOH functional group density obtained by analysis of the CO_2 TPD peak area. However, hydrogen-bonding of ammonia to ammonium carboxylate complexes was responsible for overestimation of the COOH group concentration.

By determining the mass change using a standard analytical balance after specific octadecylamine adsorption to COOH groups, Marshall et al. were able to quantify the concentration of COOH groups on SWCNTs. Using this approach, a linear correlation was observed between the quantity of COOH groups and the duration of SWCNT sonication in H_2SO_4/HNO_3, increasing from 1.9 to 7.0% over the course of 14 h of treatment time [44].

One weakness with all of the techniques described thus far is that none of them provide a sense of the spatial distribution of oxygen functional groups (and defect sites) incorporated into CNTs. This limitation has been overcome in a study by Li et al. who labeled defect sites (containing oxygen functional groups) on acid-treated SWCNTs using TiO_2 nanoparticles. An estimate of the spatial distribution of oxygen functional groups and sidewall damage sites in acid-treated SWCNTs was then possible by imaging the TiO_2 nanoparticles with AFM [45]. SWCNTs were visible in the AFM micrographs as 2–4 nm high features in contrast with the ~15 nm TiO_2 nanoparticles. The AFM micrographs showed no TiO_2 adsorption occurred on untreated SWCNTs, but after oxidation in 2.6 mol L^{-1} HNO_3, TiO_2 nanoparticles were visible on the sidewalls with an average inter-particle distance of 392 nm.

Nitrogen

The electronic and mechanical properties of CNTs can be modified by incorporating nitrogen [46, 47]. XPS has been used to assay the amount of nitrogen present in CNTs following various treatment strategies and to determine how different reaction conditions affect the concentration and bonding characteristics of the nitrogen atoms present.

For example, Arrigo et al. used XPS to quantify the amount of nitrogen (9 at. %) incorporated into MWCNTs after NH_3 treatment at 873 K, and the subsequent decrease in concentration upon *in-vacuo* heat treatment [48]. Deconvolution of the N(1s) spectral envelope showed that the nitrogen atoms were mainly incorporated in the form of pyridines, pyrroles, and lactams. As the MWCNTs were heated to 770 K, two effects were observed: a decrease in the overall nitrogen concentration and a conversion of residual nitrogen functionalities to mostly graphenic quaternary nitrogen as evidenced by changes in the N(1s) spectral envelope (Fig. 5) [48]. Furthermore, Fig. 5 illustrates that the N(1s) spectral envelope can often be unambiguously deconvoluted because of the limited number of species present, each exhibiting measurably different binding energies. Arrigo also conducted complementary TPD analysis and identified HCN, NO, and N_2 products, with HCN being the largest component. These species correspond to the thermal decomposition products of lactams and pyridine, in agreement with the changes in nitrogen speciation observed by XPS [48].

Nitrogen incorporation into SWCNTs subjected to low-energy N_2^+ implantation was studied by Xu et al. [49]. By peak-fitting the N(1s) envelope, the most prominent species were found to be sp^2-hybridized nitrogen atoms substitutionally incorporated into the graphene [49]. Morant et al. found the same results for N_2^+ bombarded SWCNTs at low nitrogen surface concentrations. In contrast, at higher nitrogen concentrations, they found that sp^3-hybridized nitrogen atoms became more prevalent [46].

Droppa et al. used XPS to study the nitrogen incorporated into MWCNTs from an arc-discharge in different partial pressures of N_2 ranging from 50 to 100% at 300 torr. Their results showed that nitrogen incorporation increased from 1.6 to 4.3 at. % as the N_2 partial pressure increased from 50 to 100% [47]. Peak fitting of the N(1s) spectral envelope indicated an increase in sp^2 hybridized nitrogen species as the atomic percentage of nitrogen increased. Using EELS in conjunction with TEM, they were also able to observe a nitrogen K edge and determined that nitrogen was only incorporated into the MWCNT sidewalls, not in the amorphous carbon that was adsorbed onto the MWCNT sidewalls [47].

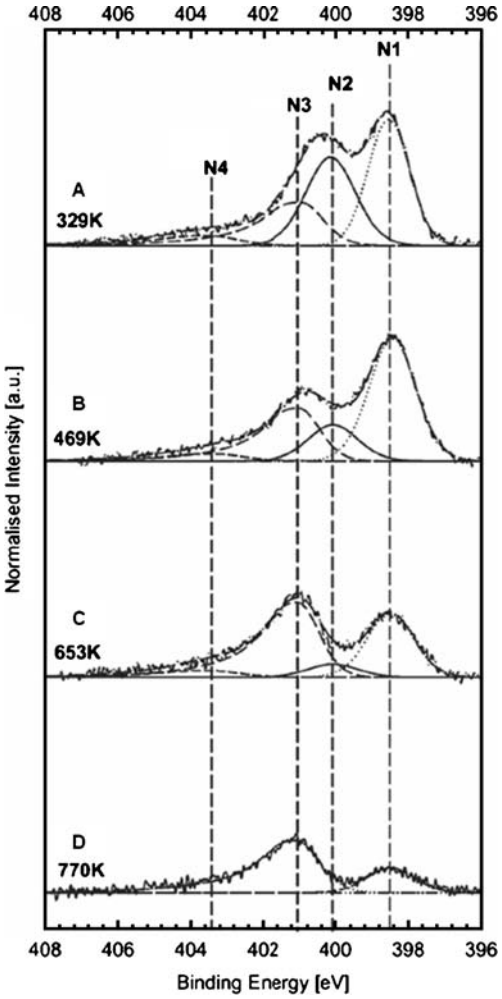

Fig. 5 N(1s) XP spectral envelopes of MWCNT treated with NH_3 at 873 K and then annealed in situ to (**A**) 329 K, (**B**) 469 K, (**C**) 653 K, and (**D**) 770 K. Four nitrogen peak positions were used to fit the N(1s) spectral envelope: N1 at 389.5 eV; N2 at 400 eV; N3 at 401.1 eV; N4 at 403.4 eV. (From Arrigo et al. [48], courtesy of The Royal Society of Chemistry, 2008)

Fluorine

Fluorination of CNTs introduces highly polar C-F bonds into the CNT sidewalls, which alter the nanomaterial's electronic properties. For example, Wang and Sherwood used XPS to show that higher levels of grafted fluorine reduce the conductivity of SWCNTs; they were also able to develop a model that predicted changes in conductivity based on the separation between the C-C peak and the C-F_x peak in the C(1s) region [50].

Fluorine atoms are often grafted into the CNT surface by exposing CNTs to F_2 at elevated temperatures. In several studies, XPS has been used to correlate the effect of exposure time to F_2 and temperature on the concentration of fluorine atoms introduced into CNT surfaces [51–53]. In terms of XPS spectral deconvolution, the high electronegativity of fluorine compared with carbon allows different

CF_x (x=0...3) species to be easily resolved from the graphenic carbon atoms on the CNTs' surfaces. In this way, Shulga et al. were able to determine that after exposing MWCNTs to F_2 gas at 420 °C, most of the species present were C-F groups. This is based on the observation of an additional peak in the C(1s) region at a binding energy of 289.4 eV compared to unmodified CNT carbon atom with C(1s) binding energies at 284.6 eV [53]. They also observed, using TEM, that highly fluorinated carbon atoms (more than one fluorine for every two carbons) were exfoliated from CNTs [53]. In a related study, An et al. found that when SWCNTs were fluorinated, the quantity of fluorine attached to the CNT sidewalls increased from 16 at. % at 150 °C to 40 at. % by 300 °C. Peak fitting of the C(1s) and F(1s) spectral envelopes indicated that as the fluorination temperature increased, the surface changes from one that consisted of isolated C-F groups to fluorine-saturated cyclohexane rings (i.e., each carbon containing a C-F bond) [52]. A subsequent TEM study by the same researchers showed that in areas of fluorination, the inter-wall spacing of the MWCNT was larger than in unfluorinated areas [52]. Marcoux et al. studied fluorination of SWCNTS with F_2 and subsequent defluorination with hydrazine using XPS and Raman [51]. They used XPS to monitor the extent of fluorine incorporation and Raman D-band intensities to show that an increase in disorder resulted from increasing fluorination (Fig. 6i), presumably as a consequence of sidewall damage. A subsequent decrease in the D-band intensity was observed after defluorination by hydrazine as the sidewall was repaired (Fig. 6ii).

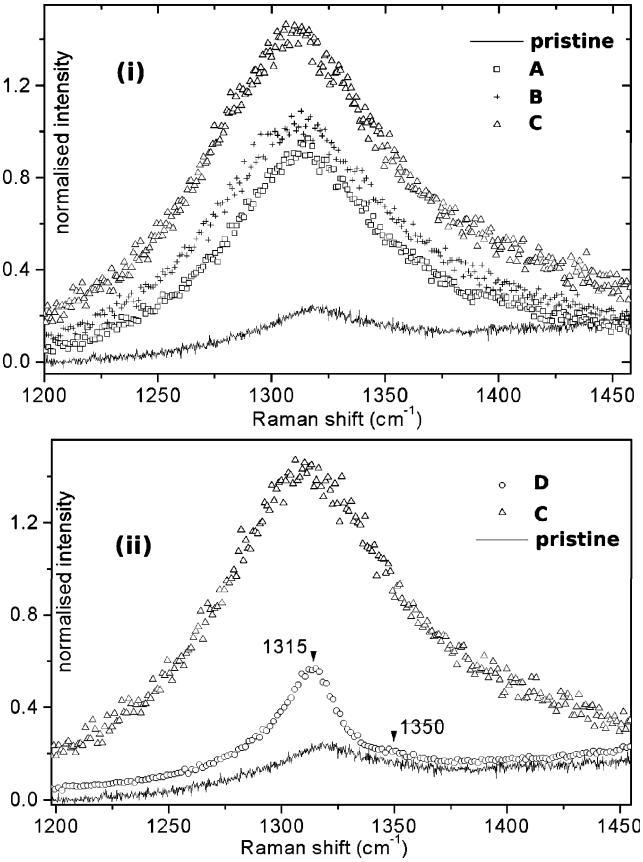

Fig. 6 Raman D bands of (**i**) SWCNTs as a function of increasing fluorine concentration (C (*triangles*) > B (*crosses*) > A (*squares*)) and (**ii**) fluorinated SWCNTs before (C (*triangles*)) and after (D (*circles*)) exposure to hydrazine. For comparison, the Raman D band of the pristine SWCNTs (*black line*) is shown in both (i) and (ii). (From Marcoux et al. [51], courtesy of The Royal Society of Chemistry, 2002)

Organic functionalization

Organic functionalization is an effective way to modify CNT properties and create more complex, multifunctional nanostructures [30]. Covalent organic functionalization often begins with incorporation of C-F groups on to the sidewall, which can subsequently be replaced by nucleophilic substitution with more complex organic functional groups. As an example, Pulikkathara et al. functionalized fluorinated SWCNTs with urea polymers and tracked the substitution of fluorine by observing a decrease in the C-F peak (289.3 eV) area in the C(1s) spectral envelope, and an increase in spectral intensity within the N(1s) region [30]. IR spectroscopy confirmed the presence of the urea polymer [30]. Upon urea incorporation, a decrease in the sidewall defect density was also observed by an attenuation in the Raman D-band intensity [30].

In another example of organic functionalization, this time with a biocompatible molecule, Bergeret et al. used XPS peak fitting of the C(1s) spectral envelop to verify a multistep PEGylation of SWCNT surfaces. Because of the discrete and well-defined number of functional groups introduced, this is an example where spectral deconvolution of the C(1s) envelope can be effective, in contrast with studies on the affects of CNT oxidation discussed earlier. For the pristine material, the C(1s) region exhibits a single peak (285.3 eV), while the PEGylated SWCNTs have three clear peaks: one associated with graphene C-C , one from the C-O groups (286.2 eV) in the PEG backbone, and one from the O-C=O group (288.7 eV) in the ester linkage associated with PEG. The presence of the PEG surface functionality was also confirmed by IR through identification of signature PEG peaks at 1733, 1223, and 1100 cm^{-1} [37].

In a study by Dossot et al., TGA and Raman spectroscopy were used in combination to confirm the covalent sidewall functionalization of SWCNTs with methoxyphenyl (PhOMe) that was incorporated by reduction of 4-methoxyphenyl hydrazine in the presence of the pristine SWCNTs [54]. TGA showed that SWCNTs functionalized with PhOMe exhibited an increased rate of

mass loss over pristine SWCNTs, consistent with the decomposition of the less thermally stable PhOMe moiety. Furthermore, by quantifying the difference in the mass loss (7.5%) between the pristine and PhOMe-functionalized CNTs they were able to determine that one PhOMe moiety had been introduced per 110 carbon atoms. Corresponding Raman spectra exhibited a measurable increase in the I_D:I_G band ratio at higher PhOMe surface coverage whereas no changes in the Raman spectra were observed at lower PhOMe coverage.

McPhail et al. attached nitroso (NO) groups to SWCNTs using electrochemical nitrosylation in KNO_2, and attached malic anhydride (MA) to the sidewalls via a Diels-Alder cycloaddition reaction [55]. IR spectroscopy was used to verify the incorporation of organic moieties on to the SWCNTs based on the appearance of a 1577 cm^{-1} mode associated with NO groups (Fig. 7b) and the 1749 and 1720 cm^{-1} modes associated with MA (Fig. 7d), neither of which are present in the pristine (Fig. 7a) or COOH-functionalized SWCNTs (Fig. 7c) [55]. Based on the mass loss of the functionalized SWCNTs measured at 700 °C by TGA, the authors were also able to estimate the functional group coverage on each SWCNT; 1:3.1 for NO-SWCNTs and 1:9.6 for MA-SWCNTs.

Gromov et al. used a combination of Raman and IR spectroscopies to monitor the incorporation of surface amine groups by first activating an oxidized SWCNT with $SOCl_2$ to form an acid chloride intermediate. This can then be reacted with ammonium carbonate to form carboxylic acid amide, followed by a Hofmann rearrangement to form a primary amine. As an alternative route to amination, the acid chloride was also subjected to a Curtius reaction using sodium azide [56]. The lack of increase in the Raman D-band indicated that the structural integrity of the SWCNT was not affected significantly during these various surface functionalization steps, and the appearance of N-C stretching modes in the 1060–1250 cm^{-1} region in IR spectroscopy indicated that amines groups had been incorporated.

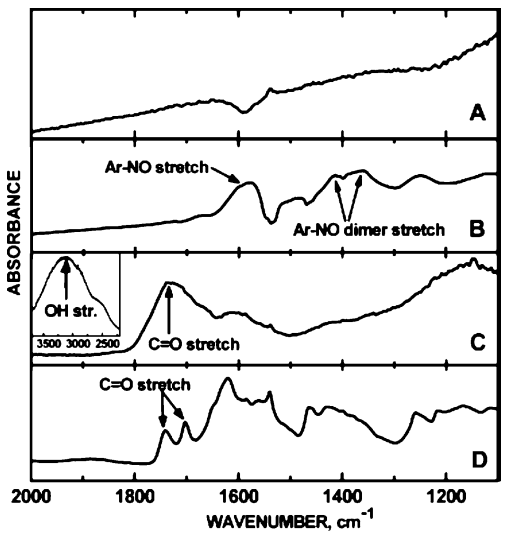

Fig. 7 IR spectra of (**A**) as-received SWCNTs; (**B**) NO-functionalized SWCNTs; (**C**) COOH-functionalized SWCNTs; and (**D**) malic anhydride (MA)-functionalized SWCNTs. (From McPhail et al. [55], Courtesy of the American Chemical Society, 2009)

Attachment of metals and metal/inorganic nanoparticles to CNT surfaces

Many CNT surface functionalization strategies involve the inclusion of metal and inorganic nanoparticles [31, 57, 58]. XPS can investigate the attachment of these nanoparticles, and in some cases, provide insight into the attachment mechanism. For example, Kocharova et al. used XPS to verify the attachment of Au nanoparticles to an SWCNT in the presence of an ionic surfactant, 1-(12-mercaptododecyl)-3-methylimidazolium bromide [57]. In a related study, Nakamura et al. attached Au nanoparticles to SWCNTs via a cyclic disulfide linker. XPS showed that the disulfide reacted with the SWCNT through C-S bond formation and liberation of a free thiol tethered to the SWCNT. Subsequently, colloidal Au nanoparticles were attached to the thiolated CNTs. XPS analysis demonstrated that the Au nanoparticles became connected to the SWCNT surface via the formation of an Au-S bond [58] that formed as a result of a reaction between the free thiol and the gold nanoparticles

XPS peak-fitting can also assist in determining speciation in metal sorption studies on to CNTs. For example, analysis of the Eu(3d) photoelectron peak positions has been used to suggest that $Eu(OH)_x$ species are the primary form of Eu(III) adsorbed by oxidized MWCNTs [59]. Similarly, Wang at al. studied Pb(II) sorption on acid washed MWCNTs and determined that most of the Pb(II) was complexed with COOH groups on the surface, based on spectral deconvolution of the O(1s) and Pb(5f) spectral envelopes [39].

Using a combination of XPS and TEM, Chetty et al. studied the reduction of Ru and Pt chloride salts on the surface of acid washed MWCNTs to form catalytic structures [31]. Analysis of Ru(3p) and Pt(4f) spectral envelopes showed that greater quantities of metal nanoparticles were produced when the reduction temperature was increased from 150 °C to 450 °C [31]. TEM analysis showed that the size of the nanoparticles also increased from 4 to 11 nm concomitantly with reduction temperature [31].

Summary

Throughout this review, we have shown how different analytical techniques can be used to study changes in the

CNTs' structure and surface chemistry as a result of covalent surface modification strategies. Clearly, each technique has its strengths and limitations. XPS, EELS, and NEAXFS can provide elemental composition, and IR can be used to identify organic functional groups present on the CNT surface. In some instances, these techniques can be used to determine the concentration of specific functional groups, but, because of ambiguities in spectral interpretation, it is sometimes necessary to employ other analytical methods such as chemical derivatization, Boehm titrations, or TPD. In terms of CNT structure, Raman spectroscopy can provide information about sidewall integrity, although without TEM, I_D:I_G band analysis can be misleading. TEM, XPS, and Raman spectroscopy are among the techniques most widely used to provide chemical and structural information about CNTs. In general, this review illustrates the fact that the best practice is to employ a complementary, multi-technique approach, where results can be verified and substantiated independently.

Acknowledgements The authors acknowledge financial support from the National Science Foundation (grant # BES0731147), the Environmental Protection Agency (grant # RD-83385701-0), and the Institute for Nanobiotechnology (INBT) at Johns Hopkins University. The authors would also like to acknowledge the Material Science Department at JHU for use of the surface analysis laboratory. Billy Smith also acknowledges support from the ARCS foundation.

References

1. Masciangioli T, Zhang W-X (2003) Environmental technologies at the nanoscale. nanotechnology could substantially enhance environmental quality and substainability through pollution prevention, treatment, and remediation. Environ Sci Technol 102A–108A
2. He X, Kitipornchai SCMW, Leiw KM (2005) Modeling of van der Waals force for infinitesimal deformation of multi-walled carbon nanotubes treated as cylindrical shells. Int J Solids Struct 42:6032–6047
3. Terrones M, Hsu WK, Kroto HW, Walton DRM (1999) Topics in current chemistry. In Nanotubes: a revolution in materials science and electronics, vol. 199. Springer Berlin / Heidelberg
4. Ebbesen TW, Lezec HJ, Hiura H, Bennett JW, Ghaemi HF, Thio T (1996) Electrical conductivity of individual carbon nanotubes. Nature 382:54–56
5. Gibson JM, Ebbensen TW, Treacy MMJ (1996) Exceptionally high Young's modulus observed for individual carbon nanotubes. Nature 381:678–680
6. Chang TE, Jensen LR, Kisliuk A, Pipes RB, Pyrz R, Sokolov AP (2005) Microscopic mechanism of reinforcement in single-wall carbon nanotube/polypropylene nanocomposite. Polymer 46:439–444
7. Ouellette J (2002/2003). Building the nanofuture with carbon tubes http://www.aip.org/tip/INPHFA/vol-8/iss-6/p18.html. The Industrial Physicist
8. Chandra B, Bhattacharjee J, Purewal M, Son Y-W, Wu Y, Huang M, Yan H, Heinz TF, Kim P, Neaton JB, Hone J (2009) Molecular-scale quantum dots from carbon nanotube heterojunctions. Nano Lett 9:1544–1548
9. Short P, McCoy M (2007) Companies invest in nanotubes. Chem Eng News 85:20
10. Cheng J, Fernando KAS, Veca LM, Sun Y-P, Lamond AI, Lam YW, Cheng SH (2008) Reversible accumulation of PEGylated single-walled carbon nanotubes in the mammalian nucleus. ACS Nano 2:2085–2094
11. Martin CR, Kohli P (2003) The emerging field of nanotube biotechnology. Nat Rev 2:29–37
12. Brundle CR, Evans CA, Wilson S (1992) Encyclopedia of materials characterization. Butterworth-Heinemann, Stoneham
13. Vickerman JC (1997) Surface analysis: the principal techniques, 1st edn. John Wiley & Sons, Chichester
14. Povstugar VI, Mikhailova SS, Shakov AA (2000) Chemical derivatization techniques in the determination of functional groups by X-ray photoelectron spectroscopy. J Anal Chem 55:455–467
15. Xing Y, Dementev N, Borguet E (2007) Chemical labeling for quantitative characterization of surface chemistry. Curr Opin Solid State Mater Sci 11:86–91
16. Boehm HP, Diehl E, Heck W, Sappok R (1964) Surface oxides of carbon. Angew Chem Int Edit 3:669–677
17. Speyer RF (1994) Thermal analysis of materials. Marcel Dekker, New York
18. Kirkland AI, Hutchison JL (eds) (2007) Nanocharacterisation. The Royal Society of Chemistry, Cambridge
19. Cho H-H, Wepasnick KA, Smith B, Bangash F, Fairbrother H, Ball W (2009). Sorption of aqueous Zn[II] and Cd[II] by multi-wall carbon nanotubes: the relative roles of oxygen-containing functional groups and graphenic carbon. Langmuir ASAP
20. Zschoerper NP, Katzenmaier V, Vohrer U, Haupt M, Oehr C, Hirth T (2009) Analytical investigation of the composition of plasma-induced functional groups on carbon nanotube sheets. Carbon 47:2174–2185
21. Dementev N, Feng X, Borguet E (2009) Fluorescence labeling and quantification of oxygen-containing functionalities on the surface of single-walled carbon nanotubes. Langmuir 25:7573–7577
22. Čech J, Kalbáč M, Curran SA, Zhang D, Dettlaff-Weglikowska U, Dunsch L, Yang S, Roth S (2007) HRTEM and EELS investigation of functionalized carbon nanotubes. Physica E 37:109–114
23. Smith BW, Luzzi DE (2001) Electron irradiation effects in single wall carbon nanotubes. J Appl Phys 90:3509–3515
24. Rao AM, Chen J, Richter E, Schlecht U, Eklund PC, Haddon RC, Venkateswaran UD, Kwon Y-K, Tománek D (2001) Effect of van der Walls interactions on the Raman modes in single walled carbon nanotubes. Phys Rev Lett 86:3895–3898
25. Itkis ME, Perea DE, Jung R, Niyogi S, Haddon R (2005) Comparison of analytical techniques for purity evaluation of single-walled carbon nanotubes. J Am Chem Soc 127:3429–3448
26. Osswald S, Flahaut E, Ye H, Gogotsi Y (2005) Elimination of D-band in Raman spectra of double-wall carbon nanotubes by oxidation. Chem Phys Lett 402:422–427
27. Osswald S, Havel M, Gogotsi Y (2007) Monitoring oxidation of multiwalled carbon nanotubes by Raman spectroscopy. J Raman Spectrosc 38:728–736
28. Yang D-Q, Rochette J-F, Sacher E (2005) Functionalization of multiwalled carbon nanotubes by mild aqueous sonication. J Phys Chem B 109:7788–7794
29. Smith B, Wepasnick K, Schrote KE, Cho H-H, Ball WP, Fairbrother DH (2009). Influence of surface oxides on the colloidal stability of multi-walled carbon nanotubes: a structure—property relationship. Langmuir 25:9767–9776
30. Pulikkathara MX, Kuznetsov OV, Khabashesku VN (2008) Sidewall covalent functionalization of single wall carbon nanotubes through reactions of fluoronanotubes with urea, guanidine, and thiourea. Chem Mater 20:2685–2695

31. Chetty R, Xia W, Kundu S, Bron M, Reinecke T, Schuhmann W, Muhler M (2009) Effect of reduction temperature on the preparation and characterization of Pt-Ru nanoparticles on multi-walled carbon nanotubes. Langmuir 25:3853–3860
32. Li M, Boggs M, Beebe TP, Huang CP (2008) Oxidation of single-walled carbon nanotubes in dilute aqueous solutions by ozone as affected by ultrasound. Carbon 46:466–475
33. Hou PX, Bai S, Yang QH, Liu C, Cheng HM (2002) Multi-step purification of carbon nanotubes. Carbon 40:81–85
34. Cho H-H, Smith BA, Wnuk JD, Fairbrother DH, Ball WP (2008) Influence of surface oxides on the adsorption of naphthalene on to multiwalled carbon nanotubes. Environ Sci Technol 42:2899–2905
35. Smith B, Wepasnick K, Schrote KE, Bertele AR, Ball WP, O'Melia C, Fairbrother DH (2009) Colloidal properties of aqueous suspensions of acid-treated, multi-walled carbon nanotubes. Environ Sci Technol 43:819–825
36. Xia W, Wang Y, Bergsträβer R, Kundu S, Muhler M (2007) Surface characterization of oxygen-functionalized multi-walled carbon nanotubes by high-resolution X-ray photoelectron spectroscopy and temperature-programmed desorption. Appl Surf Sci 254:247–250
37. Bergeret C, Cousseau J, Fernandez V, Mevellec J-Y, Lefrant S (2008) Spectroscopic evidence of carbon nanotubes' metallic character loss induced by covalent functionalization via nitric acid purification. J Phys Chem C 112:16411–16416
38. Hung NT, Anoshkin IV, Dementjev AP, Katorov DV, Rakov EG (2008) Functionalization and solubilization of thin multiwalled carbon nanotubes. Inorg Mater 44:219–223
39. Wang H, Zhou A, Peng F, Yu H, Yang J (2007) Mechanism study on adsorption of acidified multiwalled carbon nanotubes to Pb(II). J Colloid Interface Sci 316:277–283
40. Langley LA, Villanueva DE, Fairbrother DH (2006) Quantification of surface oxides on carbonaceous materials. Chem Mater 18:169–178
41. Masheter AT, Xiao L, Wildgoose GG, Crossley A, Jones JH, Compton RG (2007) Voltammetric and X-ray photoelectron spectroscopic fingerprinting of carboxylic acid groups on the surface of carbon nanotubes via derivatisation with arylnitro labels. J Mater Chem 17:3515–3524
42. Kuznetsova A, Popova I, Yates JJT, Bronikowski MJ, Huffman CB, Liu J, Smalley RE, Hwu HH, Chen JG (2001) Oxygen-containing functional groups on single-wall carbon nanotubes: NEXAFS and vibrational spectroscopic studies. J Am Chem Soc 123:10699–10744
43. Li Y-H, Wang S, Luan Z, Ding J, Xu C, Wu D (2003) Adsorption of Cadmium(II) from aqueous solution by surface oxidized carbon nanotubes. Carbon 41:1057–1062
44. Marshall MW, Popa-Nita S, Shapter JG (2006) Measurement of functionalised carbon nanotube carboxylic acid groups using a simple chemical process. Carbon 44:1137–1141
45. Li X, Niu J, Zhang J, Li H, Liu Z (2003) Labeling the defects of single-walled carbon nanotubes using titanium dioxide nanoparticles. J Phys Chem B 107:2453–2458
46. Morant C, Andrey J, Prieto P, Mendiola D, Sanz JM, Elizalde E (2006) XPS characterization of nitrogen-doped carbon nanotubes. Phys Stat Sol 6:1069–1075
47. Droppa JR, Ribeiro CTM, Zanatta AR, dos Santos MC, Alvarez F (2004) Comprehensive spectroscopic study of nitrogenated carbon nanotubes. Phys Rev B 69:045405-045401–045405-045409
48. Arrigo R, Hävecker M, Schlögl R, Su DS (2008) Dynamic surface rearrangement and thermal stability of nitrogen functional groups on carbon nanotubes. Chem Commun 4891–4893
49. Xu F, Minniti M, Barone P, Sindona A, Bonanno A, Oliva A (2008) Nitrogen doping of single walled carbon nanotubes by low energy N+/2 ion implantation. Carbon 46:1489–1496
50. Wang Y-Q, Sherwood PMA (2004) Studies of carbon nanotubes and fluorinated nanotubes by X-ray and ultraviolet photoelectron spectroscopy. Chem Mater 16:5427–5436
51. Marcoux PR, Schreiber J, Batail P, Lefrant S, Renouard J, Jacob G, Albertini D, Mevellec J-Y (2002) A spectroscopic study of the fluorination and defluorination reactions on single-walled carbon nanotubes. Phys Chem Chem Phys 4:2278–2285
52. An KH, Heo JG, Jeon KG, Bae DJ, Jo C, Yang CW, Park C-Y, Lee YH (2002) X-ray photoemission spectroscopy study of fluorinated single-walled carbon nanotubes. Appl Phys Lett 80:4235–4237
53. Shulga YM, Tien T-C, Huang C-C, Lo S-C, Muradyan VE, Polyakova NV, Ling Y-C, Loutfy RO, Moravsky AP (2007) XPS study of fluorinated carbon multi-walled nanotubes. J Electron Spectrosc Relat Phenom 160:22–28
54. Dossot M, Gardien F, Mamane V, Fort Y, Liu J, Vigolo B, Humbert B, McRae E (2007) Optical parameter to reveal the interplay between covalent functionalization and the state of aggregation of single-walled carbon nanotubes. J Phys Chem 111:12199–12206
55. McPhail MR, Sells JA, He Z, Chusuei CC (2009) Charging nanowalls: adjusting the carbon nanotube isoelectric point via surface functionalization. J Phys Chem C 113:14102–14109
56. Gromov A, Dittmer S, Svensson J, Nerushev OA, Perez-Garcia SA, Licea-Jiménez L, Rychwalski R, Campbell EEB (2005) Covalent amino-functionalisation of single-wall carbon nanotubes. J Mater Chem 15:3334–3339
57. Kocharova N, Leiro J, Lukkari J, Heinonen M, Skála T, Sutara F, Skoda M, Vondráček M (2008) Self-assembled carbon nanotubes on gold: polarization-modulated infrared reflection-absorption spectroscopy, high-resolution X-ray photoemission spectroscopy, and near-edge x-ray absorption fine structure spectroscopy study. Langmuir 24:3235–3243
58. Nakamura T, Ohana T, Ishihara M, Hasegawa M, Koga Y (2007) Chemical modification of single-walled carbon nanotubes with sulfur-containing functionalities. Diamond Relat Mater 16:1091–1094
59. Tan XL, Xu D, Chen CL, Wang XK, Hu WP (2008) Adsorption and kinetic desorption study of $^{152+154}$Eu(III) on multiwall carbon nanotubes from aqueous solution by using chelating resin and XPS methods. Radiochim Acta 96:23–29